Multiple Metal Ions Drive DNA Association by *Pvu*II Endonuclease†

Lori H. Conlan‡,§ and Cynthia M. Dupureur*,‖

Department of Chemistry and Biochemistry, University of Missouri St. Louis, St. Louis, Missouri 63121, and Department of Biochemistry and Biophysics, Texas A&M University, College Station, Texas 77843-2128

Received July 3, 2002; Revised Manuscript Received October 16, 2002

ABSTRACT: Restriction enzymes serve as important model systems for understanding the role of metal ions in phosphodiester hydrolysis. To this end, a number of laboratories have reported dramatic differences between the metal ion-dependent and metal ion-independent DNA binding behaviors of these systems. In an effort to illuminate the underlying mechanistic details which give rise to these differences, we have quantitatively dissected these equilibrium behaviors into component association and dissociation rates for the representative *Pvu*II endonuclease and use these data to assess the stoichiometry of metal ion involvement in the binding process. The dependence of *Pvu*II cognate DNA on Ca(II) concentration binding appears to be cooperative, exhibiting half-saturation at 0.6 mM metal ion and yielding an n_H of 3.5 ± 0.2 per enzyme homodimer. Using both nitrocellulose filter binding and fluorescence assays, we observe that the cognate DNA dissociation rate (k_{-1} or k_{off}) is very slow (10^{-3} s^{-1}) and exhibits a shallow dependence on metal ion concentration. DNA trap cleavage experiments with Mg(II) confirm the general irreversibility of DNA binding relative to cleavage, even at low metal ion concentrations. More dramatically, the association rate (k_1 or k_{on}) also appears to be cooperative, increasing more than 100-fold between 0.2 and 10 mM Ca(II), with an optimum value of 2.7×10^7 M^{-1} s^{-1}. Hill analysis of the metal ion dependence of k_{on} indicates an n_H of 3.6 ± 0.2 per enzyme dimer. This value is consistent with the involvement in DNA association of two metal ions per subunit active site, a result which lends new strength to arguments for two-metal ion mechanisms in restriction enzymes.

The number of metal ions involved in nucleic acid phosphodiester hydrolysis is one of the most hotly debated issues in enzyme mechanism. The most common sources of evidence for multiple-metal ion mechanisms are X-ray crystallographic studies, in which more than one metal ion is observed in enzyme−substrate complexes. These results have been reported for a number of nuclease systems, including the 3′,5′-exonuclease activity of DNA polymerase I (*1*, *2*), the hammerhead ribozyme (*3*, *4*), and a number of restriction enzymes (*5*−*9*).

While these structures are often taken as evidence of a two-metal ion mechanism, in the absence of functional analysis, this interpretation can be treacherous. The high concentrations of ligands required for crystallization can lead to occupancy of sites that may have little or no functional relevance. Further, sometimes differential behavior among the native Mg(II) and the common substitutes Mn(II) and Ca(II) is observed, increasing the potential for the misinterpretation of results (*2*, *10*).

We have therefore taken a thermodynamic solution approach to this issue, working with the small and amenable *Pvu*II endonuclease, a Mg(II)-dependent homodimeric enzyme which cleaves DNA at 5′-CAG|CTG-3′ (*11*). Applying both isothermal titration calorimetry and ^{25}Mg NMR spectroscopy to this system, we began by determining that two metal ions bind in each *Pvu*II active site with affinities that are reasonable for Mg(II) under physiological conditions (*12*, *13*). This result held for native Mg(II) as well as for Mn(II) and Ca(II). These studies provided the first support for a two-metal ion mechanism based on solution measurements. A subsequent crystallographic study confirmed the existence of two metal ion binding sites in the presence of DNA (*8*).

Despite the insights provided by this work, these results alone are not sufficient to establish or refute that these two metal ions participate in the mechanism of *Pvu*II endonuclease. To accomplish this, one must consider both binding and cleavage steps of the enzymatic reaction:

$$E + S\ (+nM) \underset{k_{-1}}{\overset{k_1}{\rightleftharpoons}} E(M)_nS \xrightarrow{k_2} E(M)_nP$$

A multiple-metal ion mechanism would involve the participation of more than one metal ion per active site in at least one of the steps of the reaction scheme.

Even when the issue of metal ion stoichiometry is neglected, the role of metal ions in DNA binding by restriction enzymes has emerged as a complex and contentious issue. In the absence of divalent metal ions, the classic *Eco*RI endonuclease forms high-affinity (picomolar) complexes with cognate DNA (*14*). Results with *Eco*RV endonuclease have been more variable. Cognate DNA dissociation

† This work was supported by the National Science Foundation (Career Award 9875917) and the Robert A. Welch Foundation (Grant A-1315).

* To whom correspondence should be addressed. Telephone: (314) 516-4392. Fax: (314) 516-5342. E-mail: cdup@umsl.edu.

‖ University of Missouri St. Louis.

§ Current address: Wadsworth Center, New York State Department of Health, Albany, NY 12201.

‡ Texas A&M University.

10.1021/bi026403o CCC: $22.00
Published on Web 11/19/2002

constants in the absence of metal ions range from picomolar to nanomolar values, depending on the conditions and methods that are used, with metal ions enhancing affinity 4−10000-fold (*15*, *16*). Indeed, the possibility that this dependence may indeed vary among restriction enzymes has been debated (*3*).

Recently, we contributed to these efforts by comparing *Pvu*II specific and nonspecific DNA binding in the presence and absence of divalent cations. While nonspecific DNA binding is essentially metal-ion independent, the addition of 10 mM Ca(II) increases the metal ion-independent cognate DNA binding affinity of *Pvu*II endonuclease by 3 orders of magnitude (*17*). This effect was observed over a wide range of conditions, implicating metal ions as being important to DNA affinity and specificity. In the first study of this type for restriction enzymes, we quantitatively extend our equilibrium DNA binding studies by resolving this behavior into its component association and dissociation rates as a function of metal ion concentration. This analysis yields evidence for a strong metal ion dependence of the enzyme−DNA association rate and the involvement of multiple metal ions in DNA binding by *Pvu*II endonuclease.

MATERIALS AND METHODS

Materials. Nitrocellulose filters (0.2 μm pore size) were purchased from Schleicher and Schuell (Keene, NH). Chelex resin was purchased from Bio-Rad (Hercules, CA). Puratronic $MgCl_2$ and $CaCl_2$ were purchased from Alfa Aesar (Ward Hill, MA). Concentrations of stock solutions were determined by flame atomic absorption spectroscopy using a Perkin-Elmer AAnalyst 700 spectrophotometer. All buffers were rendered metal-free using Chelex resin prepared as described by the vendor and verified by atomic absorption spectroscopy (*18*).

Preparation of PvuII Endonuclease. Purification of the enzyme was accomplished using phosphocellulose chromatography and heparin−Sepharose affinity chromatography as previously described (*19*). Proteins were concentrated using Amicon Centriprep and Centricon concentrators and rendered metal-free via exhaustive dialysis against metal-free buffer (*20*). All enzymes were quantitated using an ϵ_{280} of 36 900 M^{-1} cm^{-1} for the monomer subunit and subsequently expressed with respect to the dimer. Routine assays of activity were performed using HEX[1]-labeled duplexes and time-resolved fluorescence spectroscopy (*21*).

Preparation of Oligonucleotides. The unlabeled, 5′-HEX-labeled, and 5′-Cy5-labeled oligonucleotide 5′-CAGGCAGCTGCGGA-3′ and its complement were purchased desalted from IDT Technologies (Coralville, IA) and purified by PAGE and Elutrap (Schleicher and Schuell). DNA was quantitated using ϵ_{260} values provided by IDT Technologies. The contribution of the HEX dye to absorbance at 260 nm is within experimental error. All oligonucleotide concentrations are expressed with respect to the duplex. Duplexes were formed by heating to 95 °C a mixture of 1 equiv of one strand and 1 equiv of the complementary strand and permitting the sample to cool to room temperature overnight. Duplex formation was confirmed by native PAGE analysis. Samples were stored in sterile water at 4 °C for immediate use, or lyophilized for storage.

[1] Abbreviation: HEX, hexachlorofluorescein.

Where appropriate, 17 pmol of duplex DNA was radiolabeled using [γ-^{32}P]ATP (33 pmol of a 6000 Ci/mmol stock) (NEN, Boston, MA) and polynucleotide kinase (1 unit) per the manufacturer's instructions (Promega, Madison, WI). Following incubation for 2 h at 37 °C, the duplex was purified using Sephadex G-50 resin (Sigma, St. Louis, MO).

Nitrocellulose Filter Binding Assays. Filters were soaked in binding buffer immediately prior to use, backed with multiple layers of soaked filter paper, and inserted into a Slot-Blot apparatus (Bio-Rad). Arrays of 500 μL binding reaction mixtures containing fixed concentrations of radiolabeled duplex and varying concentrations of enzyme were assembled in 96-well microtiter plates and incubated as appropriate at 25 °C. A typical reaction was started by adding a mixture of enzyme and metal to DNA. The reaction mixtures were then vacuum filtered through the Slot-Blot apparatus, washed with ≈200 μL of binding buffer, and dried. Filters were then wrapped in Saran Wrap and exposed to a phosphorimager screen overnight. The resulting image was scanned on a Storm Phosphorimager and the digitized image analyzed using ImageQuant software (Molecular Dynamics, Sunnyvale, CA). Areas of intensity were selected using the ImageQuant box tool. For consistency the boxes for all selected intensities for a particular image were kept the same size. Following background correction, intensities were transferred into a Microsoft Excel file where they were normalized. Corrected intensity is defined as the signal intensity of each protein concentration minus the signal intensity where no protein is added. This value is then divided by the maximum signal intensity for a particular protein series.

Fluorescence Anisotropy. Fluorescence emission intensities were collected on an Aminco SLM 4800 spectrofluorometer equipped with a polarization assembly. The temperature was maintained with a thermostated compartment at 25 °C. HEX-labeled oligonucleotides were excited at 532 nm, and the resulting emission was passed through a 550 nm cutoff filter (Oriel, Stratford, CT) or through a monochromator set at 556 nm. The slit width was set to 4 nm. All samples were monitored with stirring using a nitric acid-cleaned quartz cuvette (NSG Scientific, Farmingdale, NY). Three readings were taken at all four combinations of vertical (v) and horizontal (h) polarizer settings using the L format, taken over a 10 s integration time, and averaged. For measurements of dissociation rate constants, the rates of decay were slow enough for this to be performed manually. Anisotropy values were calculated from the equation

$$A = (I_{||} - I_{\perp})/(I_{||} + 2I_{\perp}) \quad (1)$$

where I is the recorded intensity at the indicated polarizer positions.

Determination of the Equilibrium Constants. Equilibrium constants at $CaCl_2$ concentrations below 1 mM were weak enough to be measured spectroscopically and were therefore determined at 2.5 nM HEX-labeled 14-mer duplex using fluorescence anisotropy. Those measured above 1 mM $CaCl_2$ were obtained via nitrocellulose filter binding at 9 pM duplex. As appropriate, corrected intensities or anisotropy values (A) were then plotted versus enzyme concentration and the data fit to a simple binding isotherm (*22*) using Kaleidagraph 3.5 (Synergy, Reading, PA).

$$\theta = \frac{K_a[E]}{1 + K_a[E]} \quad (2)$$

where θ is the fraction of duplex bound, [E] is the total enzyme concentration, and K_a is the association constant.

Association and Dissociation Kinetics. Association and dissociation rates were principally measured using nitrocellulose filter binding. At specific time intervals suitable for each concentration of enzyme and metal ion, enzyme−metal stocks were added to a solution of radiolabeled duplex. The binding reaction mixtures were then filtered through a nitrocellulose filter to separate free from enzyme-bound DNA. Following densitometry, normalized intensities were plotted as a function of time and fit to the following equation to obtain k_{obs}:

$$I_t = I_\infty(1 - e^{-k_{obs}t}) \quad (3)$$

where I_t is the intensity at time t and I_∞ is the intensity at the end of the experiment. At each metal ion concentration, k_{obs} was in turn determined as a function of enzyme concentration, where the latter parameter was varied 3-fold around the K_d and the DNA concentration was at least 8-fold lower than the K_d value. At each metal ion concentration, the k_{obs} exhibits a linear dependence on enzyme concentration in which the slope is k_1 and the y-intercept is k_{-1} ($k_{obs} = k_1[E] + k_{-1}$) (*23*, *24*).

Dissociation rate constants were confirmed using competition fluorescence anisotropy. A 20-fold excess of unlabeled competitor duplex was added to a preformed complex of protein and HEX-labeled DNA and the decreasing anisotropy recorded as a function of time. To facilitate curve fitting, these data were normalized to the corrected anisotropy (or fraction bound) by subtracting the final anisotropy value from all values and dividing those by the largest remaining value. Using Kaleidagraph software, these data were fit to the equation

$$A_t = A_\infty e^{-k_{obs}t} \quad (4)$$

where t is time, A_t is the corrected anisotropy at time t, A_∞ is the corrected anisotropy of the free duplex, and k_{obs} is the observed rate constant or k_{-1}.

DNA Cleavage Experiments. DNA trap experiments were conducted to assess the reversibility of binding relative to cleavage (*25*). Given our prior knowledge of metal-free ES complex binding constants (*17*), we were able to select single-turnover conditions under which the formation of a metal-free ES complex is maximized even in the absence of metal ions. *Pvu*II endonuclease (2.5 μM dimers) and radiolabeled DNA (0.5 μM duplex) were incubated at 37 °C with Mg(II). For 1 mM Mg(II), aliquots were taken at predetermined time points between 0 and 8 min and quenched with an equal volume of unlabeled DNA (final concentration of 10 μM). The reaction mixture was incubated for an additional 8 min, and then the reaction was stopped by the addition of an equal volume of 250 mM EDTA. Reaction products were separated on a 20% polyacrylamide gel and analyzed using ImageQuant. Normalized intensities were plotted versus time and fit to eq 3 to obtain a rate constant. Under these single-turnover conditions, k_2 is the rate constant observed with EDTA-quenched reactions; k_{obs} is the rate constant observed with cold quench reactions later terminated with EDTA. k_{-1} was estimated from these data according to the equation (*25*)

$$[P]_{obs}/[P]_\infty = 0.945 = k_2/(k_2 + k_{-1}) \quad (5)$$

which relates the indicated rate constants at the observed end point of the reaction. $[P]_{obs}$ is the concentration of cleaved DNA observed when the reaction is quenched with EDTA. $[P]_\infty$ is the concentration of cleaved DNA at the end point of the reaction, which was determined from the asymptote of the fit of the data to eq 3. $[P]_{obs}/[P]_\infty$ is ideally 1.000 at the end of the reaction, but has been determined in the above fashion to be 0.945 within experimental error.

Metal Ion Dependence of Association Rate Constants. To understand how many metal ions are involved in DNA binding, the determined rate constants were fit to a form of the Hill model equation:

$$\theta = \frac{K^{n_H}[M(II)]^{n_H}}{1 + K^{n_H}[M(II)]^{n_H}} \quad (6)$$

where θ is the normalized rate constant, K is the metal ion concentration at which the rate constant is at half-maximum, n_H is the Hill coefficient, and [M(II)] is the divalent metal ion concentration.

RESULTS

Metal Ion Dependence of DNA Binding Equilibrium Constants. The goal of this study was to quantitate the participation of metal ions in site specific DNA binding by *Pvu*II endonuclease. We approached this by quantitating both equilibrium and kinetic rate constants of DNA association as a function of metal ion concentration. Because we have already established that equivalent binding constants can be obtained by either method (*17*), we used either nitrocellulose filter binding or fluorescence anisotropy as was convenient. Since Ca(II) supports DNA binding but not turnover (*26*), this metal ion was used as a substitute for Mg(II) in most experiments. The suitability of this substitution is addressed below. Since noncognate affinity has no appreciable metal ion dependence (*17*), this study involved only the cognate sequence.

As previously reported, the *Pvu*II cognate DNA binding affinity increases 3 orders of magnitude upon addition of Ca(II) (*17*). As a first step in the analysis, we expanded on this result by measuring equilibrium association constants as a function of Ca(II) ion concentration. As summarized in Figure 1, the relationship between metal ion concentration and cognate DNA affinity appears to be cooperative, exhibiting half-saturation at 0.6 mM metal ion. Hill analysis of these data yields an n_H of 3.5 ± 0.2 per enzyme dimer, consistent with the involvement of multiple metal ions per active site in DNA binding.

Effect of Metal Ion Concentration on the Association and Dissociation Rate Constants. By definition, equilibrium constants are ratios of association and dissociation rates. Do metal ions differentially affect one of these processes more than the other? If so, how many metal ions are involved, and what are the mechanistic implications? To answer these questions, we dissected the *Pvu*II cognate DNA association

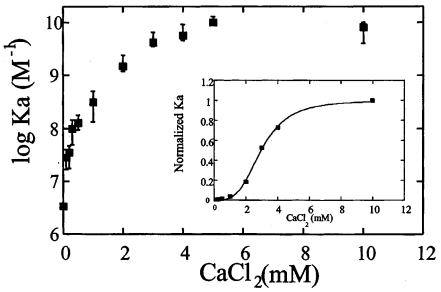

FIGURE 1: Dependence of DNA binding affinity on metal ion concentration. The conditions were 50 mM Tris, pH 7.5, and 25 °C. The NaCl concentration was adjusted to a constant ionic strength of 107.5 mM. Below 1 mM $CaCl_2$, data were collected by fluorescence anisotropy at 25 °C with 2.5 nM HEX-labeled 14-mer duplex. Above 1 mM $CaCl_2$, binding constants were measured by nitrocellulose filter binding at 9 pM DNA duplex. The inset features a Hill analysis of the data normalized on a linear scale, yielding an n_H of 3.5 ± 0.2 per enzyme dimer.

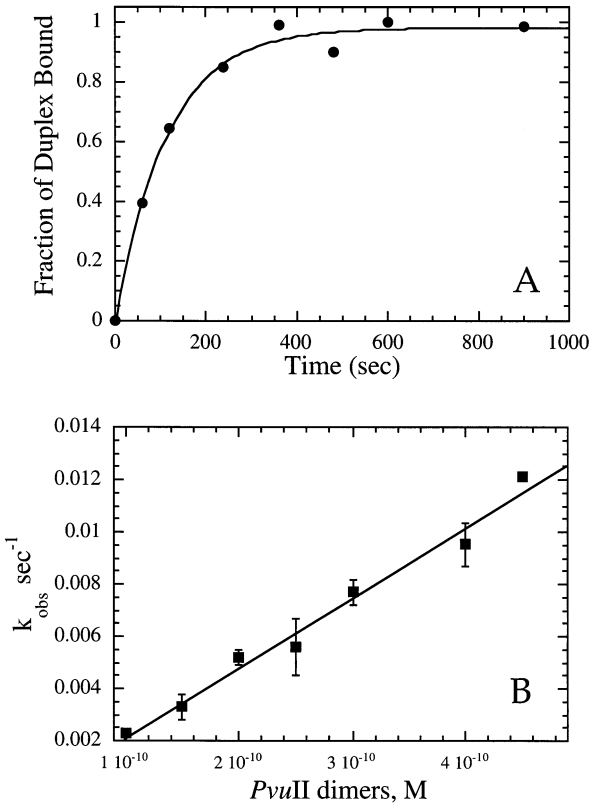

FIGURE 2: Measurement of the rate of DNA−*Pvu*II endonuclease complex formation. (A) Typical primary plot of the fraction of duplex bound vs time. The conditions were 25 °C, 50 mM Tris, pH 7.5, 77.5 mM NaCl, and 10 mM $CaCl_2$ (NaCl adjusted to an ionic strength of 107.5 mM). The duplex concentration was 40 pM, and the protein concentration was 350 pM dimers. Data were fit to a single exponential where $k_{obs} = 8.8 \times 10^{-3}$ s^{-1}. (B) Secondary plot of k_{obs} vs [E] at 10 mM $CaCl_2$. Errors represent the range of k_{obs} values obtained from multiple determinations. Linear regression analysis yields a slope (k_1) of 2.7×10^7 M^{-1} s^{-1}.

equilibrium constant into its component association (k_1) and dissociation (k_{-1}) rates as a function of metal ion concentration.

This goal was achieved using a nitrocellulose filter binding assay in which the population of enzyme-bound DNA is measured as a function of time. Figure 2A features a typical time course for these experiments. These data were fit to a single exponential to obtain an observed rate constant (k_{obs}).

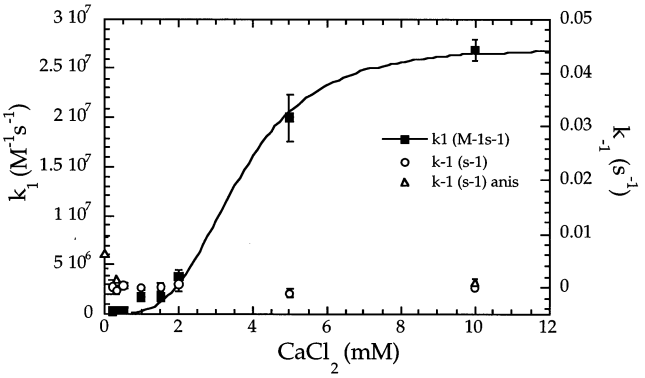

FIGURE 3: Metal ion dependence of k_1 and k_{-1}. The conditions were 50 mM Tris, pH 7.5, and 25 °C. The NaCl concentration was adjusted to a constant ionic strength of 107.5 mM: (■) k_1 obtained using nitrocellulose filter binding assays, (○) k_{-1} obtained via filter binding, and (△) k_{-1} obtained via fluorescence anisotropy. In general, errors were averaged over fits of multiple secondary plots. Hill analysis of k_1 data yielded an n_H of 3.6 ± 0.2 per enzyme dimer.

At a series of metal ion concentrations, k_{obs} was determined as a function of [E]. A typical secondary plot appears in Figure 2B. These data were then fit to the linear equation $k_{obs} = k_1[E] + k_{-1}$, where k_1 is the slope and k_{-1} the intercept (*24*). Figure 3 summarizes k_1 and k_{-1} values obtained at metal ion concentrations ranging from 0 to 10 mM $CaCl_2$. As determined by this assay, k_{-1} was centered around zero throughout the entire metal ion concentration range that was tested. In contrast, the association rate constant k_1 increases approximately 100-fold between 0.2 and 10 mM $CaCl_2$.

Dissociation Rates Measured by Competition Fluorescence Spectroscopy. To further evaluate the very slow dissociation rates and the corresponding relative metal ion independence of k_{-1} observed by nitrocellulose filter binding, we measured dissociation rate constants at a number of metal ion concentrations using competition fluorescence anisotropy. A large excess of unlabeled duplex was added to a preformed complex of enzyme and HEX-labeled DNA. Due to fluorescence detection limits, it was necessary to work at concentrations of DNA higher than that utilized for the nitrocellulose filter binding assay. The decrease in the anisotropy of the displaced HEX-labeled duplex was recorded as a function of time and fit to an exponential equation to obtain k_{-1}. Figure 4 features a typical time course for this experiment. As summarized in Table 1 and Figure 3, the dissociation rate constants obtained in this fashion are also quite small (10^{-3}−10^{-4} s^{-1}). While a perceptible metal ion dependence of k_{-1} is observed using this assay (several-fold between 0 and 10 mM $CaCl_2$), the dissociation rates measured by fluorescence spectroscopy are very slow and generally consistent with those rates observed via filter binding.

Separate measurements of equilibrium and rate constants provide an opportunity to reconcile experimentally determined values with fold changes observed for each parameter. Examination of K_d, k_1, and k_{-1} values at 0.2 and 10 mM Ca(II) reveals that within experimental error, the respective fold changes in k_1 and k_{-1} are generally consistent with fold changes in the equilibrium K_d over the same metal ion concentration range.

Binding Irreversibility versus Cleavage. The relevant mechanistic consequence of irreversible binding is that in

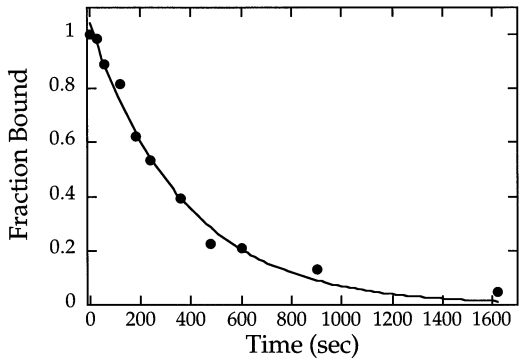

FIGURE 4: Measurement of the DNA dissociation rate using fluorescence anisotropy. The conditions were 50 mM Tris, 107.5 mM NaCl, 3 mM EDTA (metal-free), and 25 °C. To a preformed complex of 25 nM *Pvu*II dimers and HEX-labeled duplex was added unlabeled 14-mer DNA duplex to a final concentration of 500 nM. The starting and ending anisotropies were 0.1159 and 0.1036, respectively. Data were fit to a single-exponential decay as described to yield a k_{-1} of 3.42×10^{-3} s^{-1}.

Table 1: Metal Ion Dependence of DNA Dissociation Rate Constants[a]

$[CaCl_2]$ (mM)	rate constant (s^{-1})
10	$(3.87 \pm 1.20) \times 10^{-4}$
0.3	$(1.13 \pm 0.29) \times 10^{-3}$
metal-free	$(3.42 \pm 0.42) \times 10^{-3}$

[a] As monitored by fluorescence anisotropy. Rate constants calculated using an equation describing a single exponential. At 10 mM $CaCl_2$, protein dimers and HEX-labeled duplex DNA were at 2.5 nM, and unlabeled DNA was added to 175 nM duplex. At 0.3 mM $CaCl_2$, protein dimers and HEX-labeled duplex DNA were at 8 nM, and unlabeled DNA was added at 175 nM. Under metal-free conditions, the complex concentration was 25 nM and the final unlabeled DNA concentration was 500 nM. In all cases, the ionic strength was held constant at 107.5 mM in 50 mM Tris at pH 7.5 and 25 °C.

the presence of Mg(II), DNA substrates bound to enzyme are hydrolyzed rather than dissociated. To evaluate binding irreversibility relative to DNA cleavage, we conducted DNA pulse−chase or trap experiments in which unlabeled DNA competes with labeled DNA for enzyme. Using discontinuous gel electrophoresis to quantitate substrate and product, cleavage rates were compared when reactions were quenched using EDTA or using unlabeled DNA followed by EDTA. Since the Mg(II)−EDTA dissociation constant is ≈1 nM under these conditions (*27*), both free and complexed Mg(II) are subject to chelation by EDTA, leading to the observation of substrate and product distribution at the time of the quench. We compare this rate to that observed when the reaction is quenched by the addition of cold or unlabeled DNA and later by EDTA. If the binding reaction is reversible, this will lead to a dilution of the radiolabel in the EMS* complex, the observation of more uncleaved DNA, and hence an observed reaction rate that is slower than that measured with the EDTA quench (Figure 5). If the EMS* complexes are undisturbed by the addition of unlabeled substrate (irreversible binding), they will advance to cleavage well before the addition of EDTA. Figure 6 depicts reaction progress when the reaction is quenched with EDTA. Also shown in Figure 6 is a progress curve illustrating that the cold quenched reactions continue to form product until EDTA is added, exhibiting a faster observed rate. As summarized in Table 2, this pattern was observed at different Mg(II) concentrations. This indicates that relative to cleavage,

Table 2: Rates Determined from DNA Trap Experiments[a]

$[MgCl_2]$ (mM)	k_2 (s^{-1}) EDTA quench	k_{obs} (s^{-1}) cold quench	calculated k_{-1} (s^{-1})
1	2.5×10^{-2}	≥0.11	1.8×10^{-3}
0.3	5.6×10^{-3}	≥0.06	4.0×10^{-4}

[a] The conditions were 50 mM Tris, 107.5 mM NaCl, and pH 7.5. The protein concentration was 2.5 μM dimers at 1 mM $MgCl_2$ and 8 μM dimers at 0.3 mM $MgCl_2$. The DNA concentration was 0.5 μM duplex. The reaction was started by the addition of a protein−Mg(II) complex. k_2 was calculated as described in the text. k_{obs} was also obtained from a fit of the data but, because of the limited number of early points, is reported as a lower limit of the rate constant. k_{-1} was estimated from eq 5 as described in the text.

the binding reaction is essentially irreversible, even at low Mg(II) concentrations. As described above, k_{-1} was estimated from eq 5 to be 4.0×10^{-4} s^{-1} at 0.3 mM Mg(II) and 1.8×10^{-3} s^{-1} at 1 mM Mg(II). As highlighted in Table 2, these values are remarkably consistent with dissociation rates obtained via filter binding in the presence of Ca(II). This not only confirms the general observation of binding irreversibility but also indicates that Ca(II) is a suitable substitute for Mg(II) in these experiments.

DISCUSSION

The involvement of metal ions in the catalytic hydrolysis of nucleic acids is easy to accept. They are required for cleavage by restriction endonucleases, and plausible mechanisms for either one- or two-metal ion mechanisms can be readily drawn. However, hydrolysis is just one part of the mechanism; substrate binding is also a critical part of the enzymatic reaction, and metal ions can easily participate in this process as well. In many respects, involvement in DNA binding is just as complex. Equilibrium binding behavior is actually composed of both association and dissociation kinetic processes, each of which may have its own metal ion dependence. Thus, if we are to truly understand the metal ion-dependent nuclease mechanism, we must include examination of these processes and the roles of metal ions in them.

Metal ion stoichiometry issues aside, the involvement of metal ions in DNA binding by restriction enzymes has proven to be a complicated issue. This is largely due to the fact that depending on the system, conditions, and assay that were used, the reported fold enhancements in DNA binding affinity by metal ions vary widely (*15*, *16*). Due to some advances in methodology and an increase in the number of systems under study, it is becoming more generally accepted that metal ions indeed stimulate restriction enzyme affinity for DNA (*17*, *28*). With this establishment comes the challenge to understand how metal ions contribute to this process. Do metal ions participate in the formation of the enzyme−DNA complex, its dissociation, or both? What is the stoichiometry of metal ion involvement in these processes? To answer these important mechanistic questions, we dissected the metal ion dependence of the *Pvu*II DNA equilibrium constant into the component kinetic rate constants.

DNA Association and Dissociation Rates. It is generally held that most enzyme−substrate complexes optimally associate at 10^7 M^{-1} s^{-1}, a rate near the diffusion-controlled limit for such specific complexes (*29*). With oligonucleotide substrates, association rates among nucleic acid enzymes are

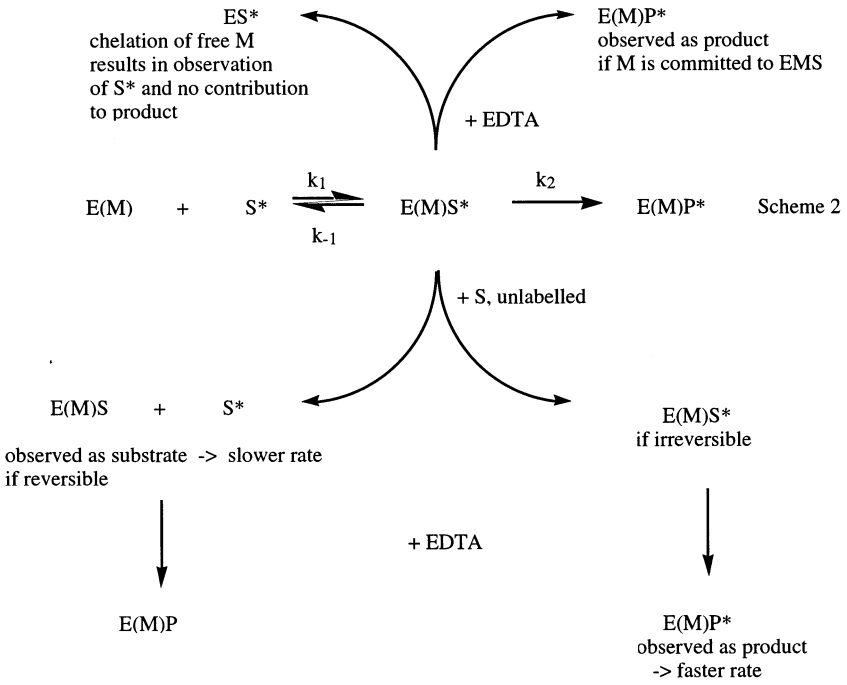

FIGURE 5: DNA trap experimental scheme which outlines the observation of substrate or product when the cleavage reaction is quenched by EDTA or unlabeled DNA duplex.

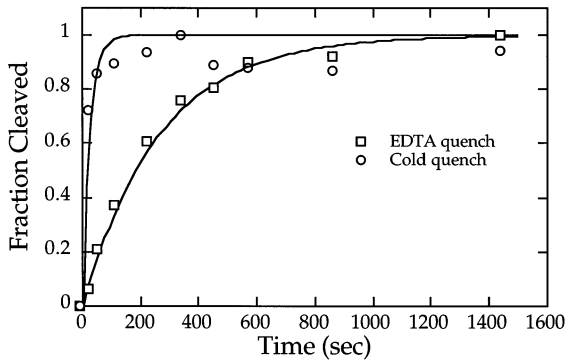

FIGURE 6: Time course for a representative DNA trap reaction. ^{32}P- or Cy-5-labeled 14-mer DNA (0.5 μM) was mixed with protein (8 μM) and 0.3 mM Mg(II) at 37 °C. The reaction was quenched by the addition of EDTA to 90 mM (□) or 20 μM unlabeled DNA (○). EDTA was added to the unlabeled DNA quench after 8 min. Reaction products were analyzed after gel electrophoresis. The data were fit to a single-exponential model and analyzed as described in the text.

typically 10^7-10^8 M^{-1} s^{-1} (*30*−*32*). Reported rates for restriction enzymes range from 10^5 to 10^8 M^{-1} s^{-1} (*33*−*35*). Our measured association rate of 10^7 M^{-1} s^{-1} for *Pvu*II endonuclease in 10 mM $CaCl_2$ is consistent with these trends and indicates that the enzyme is associating optimally under these conditions.

Multiple methods were applied to assess the dissociation constant for the cognate DNA−*Pvu*II endonuclease complex. Nitrocellulose filter binding yielded k_{-1} values that centered around zero and never exceeded 10^{-3} s^{-1}. Since these values were obtained from the *y*-intercepts of plots of k_{obs} versus [E] and therefore were especially sensitive to experimental error, we confirmed these values with two other methods. The first, competition fluorescence anisotropy, yielded values in approximately the same range. This is consistent with what is known about DNA dissociation rates for restriction enzymes. *Eco*RI endonuclease exhibits an off-rate of 7.5 × 10^{-4} s^{-1} (*36*). *Taq*I endonuclease was also shown to exhibit irreversible DNA binding behavior (*37*).

To evaluate dissociation rates in the context of cleavage, k_{-1} was estimated from DNA trap experiments in which Mg(II) was a cofactor. In this case as well, k_{-1} was determined to be much slower than the chemical step (k_2) and consistently slow ($10^{-3}-10^{-4}$ s^{-1}) at multiple metal ion concentrations. Thus, it appears that Ca(II) and Mg(II) behave similarly in supporting *Pvu*II DNA binding behavior. Further, cognate DNA binding is essentially irreversible; i.e., once the E(M)S complex forms, the species is committed to product formation. Since cleavage of unmethylated foreign DNA is critical to function, it seems advantageous for the enzyme to complete cleavage before dissociating.

Metal Ion Dependence of DNA Association Kinetics. The metal ion dependence of equilibrium DNA binding provides a valuable opportunity to measure and utilize association and dissociation rate constants to define the role of metal ions in *Pvu*II complex formation. As summarized in Figure 3, k_{-1} exhibits very little dependence on Ca(II) concentration. Using fluorescence anisotropy, the dissociation rate exhibits a shallow dependence on metal ion concentration, producing a several-fold difference between 0 and 10 mM $CaCl_2$. Thus, metal ions have a modest reducing effect on *Pvu*II−DNA dissociation rates. There is little information available regarding this behavior in other systems. However, when dissociation rates were estimated from published $t_{1/2}$ data for *Eco*RV endonuclease, the presence of 5 mM Ca(II) was also found to retard complex dissociation relative to metal-free conditions (*15*).

In stark contrast, Figure 3 highlights the more dramatic influence of metal ions on DNA association by *Pvu*II endonuclease. In this case, association rates increase approximately 100-fold between 0.2 and 10 mM Ca(II). While there are very few studies as quantitative as the one presented here, there is some variety regarding the metal ion depen-

dence of protein−nucleic acid binding. The interaction of RNaseP with its tRNA substrate shows that metal ions significantly influence the complex dissociation rate, not the association rate (*23*). The authors suggest that the metal ion dependence of k_{-1} indicates that metal ions are bound after the formation of the enzyme−tRNA complex. The opposite effect observed for *Pvu*II endonuclease suggests that it is kinetically advantageous for DNA to bind to the preformed EM complex as opposed to the free enzyme. Since *Pvu*II dissociation rates are so slow, there would be little benefit to slowing them further with a cofactor. Primarily on the basis of the order of addition experiments, there is some evidence for similar behavior by *Eco*RV endonuclease (*38*).

To put this result into some energetic context, recent studies involving specific protein−protein interactions suggest that dissociation rates are dependent upon short-range interactions (including hydrogen bonds and van der Waals interactions) but are independent of ionic strength and thus long-range interactions (*39*). If this extends to protein−nucleic acid interactions and thus to *Pvu*II endonuclease, then the lack of a strong metal ion dependence of k_{-1} indicates that other, short-range interactions at the enzyme−DNA interface dictate the very slow dissociation rates. Conversely, association rates are directly proportional to electrostatic interaction energies (*40*). This makes the metal ion dependence of k_1 easy to rationalize. Divalent cations neutralize the negative charge in the active site and generate a more favorable electrostatic interface between the enzyme and the DNA. However, it is important to emphasize that since our observations were made at a constant ionic strength, this effect is specific to the divalent cation rather than attributable to nonspecific screening effects.

Involvement of Multiple Metal Ions in DNA Binding. The issue of one- versus multiple-metal ion mechanisms for nucleases continues to receive detailed attention. The debate extends from the 3′,5′-exonuclease activity of DNA polymerase I (*1*, *2*) to ribozymes (*3*, *4*, *41*, *42*) and restriction enzymes (*43*). Proposals for two-metal ion mechanisms for the latter group have emerged primarily from X-ray crystallographic studies (*5*, *6*, *44*, *45*). Although active site coordination ligands and metal ions used in the studies vary, crystallographers report that electron densities are consistent with the presence of two metal ions in enzyme active sites. Whether this translates into two metal ions being involved in the mechanism continues to be the subject of some debate (*10*, *46*).

Due largely to the multitude of techniques that have been applied, the case for a two-metal ion mechanism for *Pvu*II endonuclease is becoming more compelling. First, using calorimetric and NMR spectroscopic techniques, we thermodynamically characterized two metal ion binding sites per *Pvu*II active site (*12*, *17*). The subsequent publication of the crystal structure of *Pvu*II endonuclease complexed to DNA and two metal ions per active site provided additional support (*8*).

The quantitative data collected here provide a unique opportunity to determine the number of metal ions involved in the kinetics of DNA binding by *Pvu*II endonuclease. Hill analysis of the k_1 data in Figure 3 yields an n_H of 3.6 ± 0.2. While the experiments presented here were not designed to address the location of the metal ions that are involved, it is consistent with the participation of at least four metal ions per enzyme dimer or two metal ions per subunit active site. Note that this value is very similar to the Hill number obtained above from the metal ion dependence of the equilibrium constant. This consistency lends strong support not only to the measurements but also to the assessment that it is the metal ion involvement in DNA association that dominates the mechanism of binding. Further, these results are wholly consistent with our previous thermodynamic detection of two metal ion binding sites per monomer active site (*12*, *13*).

The apparent cooperative nature of the metal ion dependence of DNA binding begs some consideration regarding its structural significance. There has been some discussion about conformational adjustments associated with the establishment of a competent EMS complex (*38*) as well as suspicion about the role of intersubunit articulation in enzyme function (*43*, *44*). The data presented here might be consistent with one or both of these behaviors. A simple interpretation of the observed cooperative behavior is that as metal ion binding sites are filled, reactant groups necessary for binding and cleavage become optimally arranged. Further, it is clear from the data that maximum binding activity is achieved when multiple metal ions are in place. The order in which the sites are filled and how they are linked are questions left for future investigations.

In conclusion, we have conducted the first quantitative dissection of the metal ion dependence of DNA binding kinetics. Further, we have established the kinetic advantage of ordered binding, with DNA binding to the preformed EM complex. Most importantly, the metal ion dependence of DNA binding supports the involvement of multiple metal ions in *Pvu*II endonuclease function.

ACKNOWLEDGMENT

We are grateful to Carol Fierke, Don Pettigrew, and Nancy Horton for helpful discussions.

REFERENCES

1. Steitz, T. A., and Steitz, J. A. (1993) *Proc. Natl. Acad. Sci. U.S.A. 90*, 6498−6502.
2. Black, C. B., and Cowan, J. A. (1998) *J. Biol. Inorg. Chem. 3*, 292−299.
3. Lott, W. B., Pontius, B. W., and von Hippel, P. H. (1998) *Proc. Natl. Acad. Sci. U.S.A. 95*, 542−547.
4. Zhou, D.-M., Kumar, P. K. R., Zhang, L.-H., and Taira, K. (1996) *J. Am. Chem. Soc. 118*, 8969−8970.
5. Kostrewa, D., and Winkler, F. K. (1995) *Biochemistry 34*, 683−696.
6. Newman, M., Lunnen, K., Wilson, G., Greci, J., Schildkraut, I., and Phillips, S. E. V. (1998) *EMBO J. 17*, 5466−5476.
7. Viadiu, H., and Aggarwal, A. K. (1998) *Nat. Struct. Biol. 5*, 910−916.
8. Horton, J. R., and Cheng, X. (2000) *J. Mol. Biol. 300*, 1049−1056.
9. Chevalier, B. S., Monnat, R. J., and Stoddard, B. L. (2001) *Nat. Struct. Biol. 8*, 312−316.
10. Cowan, J. A. (1997) *J. Biol. Inorg. Chem. 2*, 168−176.
11. Gingeras, T. R., Greenough, L., Schildkraut, I., and Roberts, R. J. (1981) *Nucleic Acids Res. 9*, 4525−4536.
12. José, T. J., Conlan, L. H., and Dupureur, C. M. (1999) *J. Biol. Inorg. Chem. 4*, 814−823.
13. Dupureur, C. M., and Conlan, L. H. (2000) *Biochemistry 39*, 10921−10927.
14. Jen-Jacobson, L., Kurpiewski, M., Lesser, D., Grable, D., Boyer, H. W., Rosenberg, J. M., and Greene, P. J. (1983) *J. Biol. Chem. 258*, 14638−14646.

15. Engler, L. E., Welch, K. K., and Jen-Jacobson, L. (1997) *J. Mol. Biol. 269*, 82−101.
16. Martin, A. M., Horton, N. C., Lusetti, S., Reich, N. O., and Perona, J. J. (1999) *Biochemistry 38*, 8430−8439.
17. Conlan, L. H., and Dupureur, C. M. (2002) *Biochemistry 41*, 1335−1342.
18. Holmquist, B. (1988) *Methods Enzymol. 158*, 6−12.
19. Dupureur, C. M., and Hallman, L. M. (1999) *Eur. J. Biochem. 261*, 261−268.
20. Wagner, F. W. (1988) *Methods Enzymol. 158*, 21−32.
21. Lee, S. P., and Han, M. K. (1997) *Methods Enzymol. 278*, 343−363.
22. Heyduk, T., and Lee, J. C. (1990) *Proc. Natl. Acad. Sci. U.S.A. 87*, 1744−1748.
23. Beebe, J. A., and Fierke, C. A. (1994) *Biochemistry 33*, 10294−10304.
24. Bernasconi, C. F. (1976) *Relaxation Kinetics*, Academic Press, New York.
25. Rose, I. A. (1980) *Methods Enzymol. 64*, 47.
26. Nastri, H. G., Evans, P. D., Walker, I. H., and Riggs, P. D. (1997) *J. Biol. Chem. 272*, 25761−25767.
27. Martell, A. E., and Smith, R. M. (1989) *Critical Stability Constants*, Plenum, New York.
28. Reid, S. L., Parry, D., Liu, H.-H., and Connolly, B. A. (2001) *Biochemistry 40*, 2484−2494.
29. Hammes, G. G., and Schimmel, P. R. (1970) *The Enzymes: Kinetics and Mechanism* (Boyer, P. D., Ed.) Vol. 2, pp 67−114, Academic Press, New York, NY.
30. Otto, M. R., Bloom, L. B., Goodman, M. F., and Beecham, J. M. (1998) *Biochemistry 37*, 10156−10163.
31. Strauss, P. R., Beard, W. A., Patterson, T. A., and Wilson, S. H. (1997) *J. Biol. Chem. 272*, 1302−1307.
32. Kruhoffer, M., Urbanke, C., and Grosse, F. (1993) *Nucleic Acids Res. 21*, 3943−3949.
33. Erksine, S. G., Baldwin, G. S., and Halford, S. E. (1997) *Biochemistry 36*, 7567−7576.
34. Hensley, P., Nardone, G., Chirikjian, J. G., and Wastney, M. E. (1990) *J. Biol. Chem. 265*, 15300−15307.
35. Jen-Jacobson, L., Lesser, D., and Kurpiewski, M. (1986) *Cell 45*, 619−629.
36. Jack, W. E., Terry, B. J., and Modrich, P. (1982) *Proc. Natl. Acad. Sci. U.S.A. 79*, 4010−4014.
37. Zebala, J. A., Choi, J., and Barany, F. (1992) *J. Biol. Chem. 267*, 8097−8105.
38. Baldwin, G. S., Sessions, R. B., Erskine, S. G., and Halford, S. E. (1999) *J. Mol. Biol. 288*, 87−103.
39. Selzer, T., Albeck, S., and Schreiber, G. (2000) *Nat. Struct. Biol. 7*, 537−541.
40. Selzer, T., and Schreiber, G. (1999) *J. Mol. Biol. 287*, 409−419.
41. Weinstein, L. B., Jones, B. C. N. M., Cosstick, R., and Cech, T. R. (1997) *Nature 388*, 805−808.
42. Shan, S., Kravchuk, A., Piccirilli, J., and Herschlag, D. (2001) *Biochemistry 40*, 5161−5171.
43. Pingoud, A., and Jeltsch, A. (2001) *Nucleic Acids Res. 29*, 3705−3727.
44. Newman, M., Strzelecka, T., Dorner, L. F., Schildkraut, I., and Aggarwal, A. K. (1995) *Science 269*, 656−663.
45. Horton, N. C., and Perona, J. J. (2001) *Nat. Struct. Biol. 8*, 290−293.
46. Groll, D. H., Jeltsch, A., Selent, U., and Pingoud, A. (1997) *Biochemistry 36*, 11389−11401.

BI026403O